Potent Gene-Specific Inhibitory Properties of Mixed-Backbone Antisense Oligonucleotides Comprised of 2′-Deoxy-2′-fluoro-D-arabinose and 2′-Deoxyribose Nucleotides[†,#]

Chun-Nam Lok,[‡,§] Ekaterina Viazovkina,[||] Kyung-Lyum Min,[‡] Eva Nagy,[‡] Christopher J. Wilds,[||] Masad J. Damha,*[,||] and Michael A. Parniak*[,‡,§,⊥]

Lady Davis Institute for Medical Research, Department of Medicine, and Department of Chemistry, McGill University, Montreal, Quebec PQ, Canada H3A 2K6

Received July 19, 2001

ABSTRACT: Phosphorothioate deoxyribonucleotides (PS-DNA) are among the most widely used antisense inhibitors. PS-DNA exhibits desirable properties such as enhanced nuclease resistance, improved bioavailability, and the ability to induce RNase H mediated degradation of target RNA. Unfortunately, PS-DNA possesses a relatively low binding affinity for target RNA that impacts on its potency in antisense applications. We recently showed that phosphodiester-linked oligonucleotides comprised of 2′-deoxy-2′-fluoro-D-arabinonucleic acid (FANA) exhibit both high binding affinity for target RNA and the ability to elicit RNase H degradation of target RNA [Damha et al. (1998) *J. Am. Chem. Soc. 120*, 12976]. In the present study, we evaluated the antisense activity of phosphorothioate-linked FANA oligonucleotides (PS-FANA). Oligonucleotides comprised entirely of PS-FANA were somewhat less efficient in directing RNase H cleavage of target RNA as compared to their phosphorothioate-linked DNA counterparts, and showed only weak antisense inhibition of cellular target expression. However, mixed-backbone oligomers comprised of PS-FANA flanking a central core of PS-DNA were found to possess potent antisense activity, inhibiting specific cellular gene expression with EC_{50} values of less than 5 nM. This inhibition was a true antisense effect, as indicated by the dose-dependent decrease in both target protein and target mRNA. Furthermore, the appearance of mRNA fragments was consistent with RNase H mediated cleavage of the mRNA target. We also compared a series of PS-[FANA-DNA-FANA] mixed-backbone oligomers of varying PS-DNA core sizes with the corresponding 2′-*O*-methyl oligonucleotide chimeras, i.e., PS-[2′meRNA-DNA-2′meRNA]. Both types of oligomers showed very similar binding affinities toward target RNA. However, the antisense potency of the 2′-*O*-methyl chimeric compounds was dramatically attenuated with decreasing DNA core size, whereas that of the 2′-fluoroarabino compounds was essentially unaffected. Indeed, a PS-FANA oligomer containing a single deoxyribonucleotide residue core retained significant antisense activity. These findings correlated exactly with the ability of the various chimeric antisense molecules to elicit RNase H degradation of the target RNA in vitro, and suggest that this mode of inhibition is likely the most important determinant for potent antisense activity.

Antisense oligonucleotides (AONs)[1] are rationally designed modulators of gene expression with applications in functional genomics, drug target validation, and human therapeutics (*1*−*4*). AONs are short synthetic oligomers that are designed to hybridize to a specific sequence of a given mRNA target through Watson−Crick base-pairing interactions, thereby interfering with expression of the encoded protein. An ideal antisense molecule should possess chemical stability and nuclease resistance—properties favorable for cell availability—and good affinity for binding to the RNA target. In addition, the inhibitory potency of antisense agents seems to correlate with their ability to elicit ribonuclease H (RNase H) degradation of the RNA target. RNase H is a ubiquitous cellular enzyme that specifically degrades the RNA strand of DNA/RNA hybrids (*1*, *2*, *5*) and thereby inactivates the mRNA toward further cellular metabolic processes.

[†] This work was supported in part by a grant from the Canadian Institutes of Health Research (M.A.P. and M.J.D.) and funding from Anagenis, Inc. [Montreal, QC; supported by MedTech Partners and Transfer Technology Commercialization Capital (T2C2/BIO)]. M.A.P. and M.J.D. are principals in Anagenis, Inc. During the conduct of this research, M.A.P. was a CIHR Senior Scientist and an International Research Scholar of the Howard Hughes Medical Institute.

* Corresponding authors. M.J.D.: Department of Chemistry, McGill University, 801 Sherbrooke St. W., Montreal, QC, Canada H3A-2K6. Tel: (514) 398-7552, Fax: (514) 398-3797, Email: masad.damha@mcgill.ca.

[#] This work is dedicated to Professor David N. Harpp on the occasion of his 65th birthday.

[‡] Lady Davis Institute for Medical Research.

[§] Department of Medicine.

[||] Department of Chemistry.

[⊥] Present address: University of Pittsburgh School of Medicine, Department of Medicine, Division of Infectious Diseases, Scaife Hall, Room S818D, 3550 Terrace St., Pittsburgh, PA 15261. Tel: (412) 648-1927, Fax: (412) 383-7982, Email: parniakm@msx.dept-med.pitt.edu.

[1] Abbreviations: AON, antisense oligonucleotide; ANA, arabinonucleic acid; FANA, 2′-deoxy-2′-fluoro-D-arabinonucleic acid; PS-DNA, phosphorothioate deoxyribonucleic acid; PS-FANA, phosphorothioate FANA; PS-FANA-DNA-FANA, a chimeric phosphorothioate PS-FANA oligomer containing a central DNA core; PS-2′meRNA-DNA-2′meRNA, a chimeric 2′-*O*-methyl PS-RNA oligomer containing a central DNA core; k_{rel}, relative pseudo-first-order decay constant; RNase H, ribonuclease H; T_m, melting temperature; X1/5 cells, HeLa cervical carcinoma cells stably transfected with a luciferase gene.

10.1021/bi0115075 CCC: $22.00
Published on Web 02/13/2002

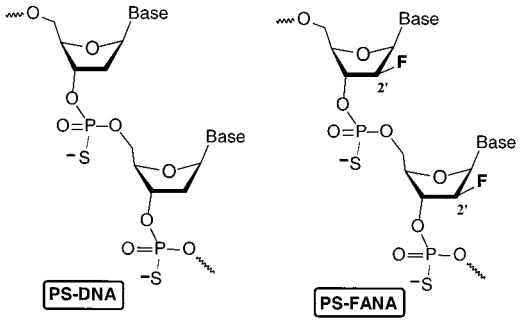

FIGURE 1: Structures of PS-FANA and PS-DNA.

Phosphorothioate DNA (PS-DNA) oligonucleotides have many properties important for antisense use, and are among the most widely used type of AON molecule. This widespread use stems from their ability to support RNase H-assisted hydrolytic cleavage of target RNA (*1, 2*); however, this activity is somewhat impaired due to their lower binding affinities. Accordingly, much effort in antisense development has been directed at developing new AON structures with improved binding affinity for target RNA. AONs possessing 2′-modifications of the sugar moiety have received considerable attention. For example, 2′-*O*-alkyl RNA shows dramatic increases in binding affinity to target RNA compared to PS-DNA and even to phosphodiester-linked DNA and RNA (*6, 7*). Unfortunately, 2′-*O*-alkyl RNA does not elicit RNase H degradation of target RNA (*8*), which limits its usefulness as an antisense agent.

Current antisense technology involves mixed-backbone AONs comprising 2′-*O*-alkyl RNA flanking a central DNA core. These "chimeric" AONs can be potent inhibitors, since they form stable duplexes with RNA and exhibit nuclease resistance via the 2′-*O*-alkyl RNA "wings" at the 3′- and 5′-ends of the molecule; they also elicit RNase H degradation of the target RNA via the central DNA core (*9*−*13*). Nonetheless, these AONs are less than ideal, since efficient RNase H cleavage of target RNA requires a DNA core of at least eight nucleotides.

Recently, we showed that the stereochemistry at the 2′-position of the sugar of antisense oligonucleotides is a key determinant in the target RNA binding affinity and the activation of RNase H (*14*−*17*). We demonstrated that both arabinonucleic acid (ANA), the 2′-epimer of RNA, and the corresponding 2′-deoxy-2′-fluoro-D-arabinonucleic acid analogue (FANA, Figure 1) form hybrids with RNA, and are able to induce RNase H degradation of the target RNA (*14*). While ANA has only relatively weak binding affinity for an RNA complement (*15*), FANA/RNA hybrids exhibit high thermal stabilities (*14, 16*). FANA represents the first example of a fully 2′-modified nucleic acid that both has high-affinity RNA binding and can retain RNase H cleavage properties, suggesting that FANA may demonstrate potent intracellular antisense activity.

The present report describes the antisense characteristics of oligonucleotides based on phosphorothioate FANA (PS-FANA), and of mixed-backbone (chimeric) AONs of the general structure PS-[FANA-DNA-FANA]. The latter were found to have exceptionally potent antisense activity. The antisense activities of the 2′-fluoroarabino chimeras were sequence-specific and mediated by intracellular RNase H (human). Importantly, unlike 2′-*O*-methylribose chimeric compounds, the potencies of the 2′-fluoroarabino chimeras were not limited by the size of the DNA core. Our results indicate that antisense-directed RNase H degradation of the target RNA is the single most important determinant for the gene-specific inhibitory potency of an antisense oligonucleotide.

MATERIALS AND METHODS

Oligonucleotide Synthesis. Fluoroarabinonucleoside monomers were synthesized as previously described (*15*). PS-FANA and PS-[FANA-DNA-FANA] chimeras were synthesized on a 1 μmol scale using an Expedite 8909 DNA synthesizer. Long-chain alkylamine controlled-pore glass (LCAA-CPG) was used as the solid support. The synthesis cycle consisted of the following steps: (a) Detritylation of nucleoside/tide bound to CPG (3% trichloroacetic acid/dichloromethane), 150 s; (b) coupling of 2′-F-arabinonucleoside or 2′-deoxyribonucleoside 3′-phosphoramidite monomers, 15 min; the concentrations of monomers used were 50 mg/mL for araF-T, araF-C, and DNA monomers, and 60 mg/mL for araA and araF-G (acetonitrile as solvent); (c) acetylation using the standard capping step, 20 s; the capping solution consisted of 1:1 (v/v) of "cap A" and "cap B" reagents (cap A: acetic anhydride/collidine/THF, 1:1:8; cap B: *N*-methylimidazole/THF, 4:21); (d) extensive washing with acetonitrile (50 pulses); (e) sulfuration with a fresh solution of 0.2 M 3*H*-1,2-benzodithiol-3-one in acetonitrile, 10 min; (f) washing with acetonitrile, 20 pulses; (g) drying of the solid support by addition of the capping reagent (see step 3), 5 s; (h) washing with acetonitrile (20 pulses).

Following chain assembly, oligonucleotides were cleaved from the solid support and deprotected as previously described (*15*). The crude oligomers were purified by either (a) preparative gel electrophoresis (24% acrylamide, 7 M urea) followed by desalting (Sephadex G-25) or (b) anion-exchange HPLC followed by desalting (SepPak cartridges); yields, 5−30 A_{260} units. Conditions for HPLC purification were as follows: column, Protein Pak DEAE-5PW (7.5 mm × 7.5 cm, Waters); solvents, buffer A: H_2O, buffer B: 1 M $NaClO_4$; gradient, 100% buffer A isocratic for 12 min, 100% A to 15% B, linear (over 5 min), 15% B to 55% B, linear (over 60 min); flow rate, 1 mL/min; temperature, 50 °C. The detector was set at 260 nm for analytical and at 290 nm for preparative chromatography. Under these conditions, the desired full-length oligomer eluted last.

Phosphorothioated DNA (PS-DNA) and PS-[2′meRNA-DNA-2′meRNA] chimeras were obtained commercially from the University of Calgary DNA Synthesis Laboratory (Calgary, ALTA). They were purified (HPLC) and desalted (SepPak cartridges) as described above. The base sequence and hybridization properties of the various oligonucleotides synthesized are given in Table 1. This antisense sequence (ATA TCC TTG TCG TAT CCC) is complementary to a coding region of luciferase mRNA sequence (+1056 to +1073; where the published transcriptional start site is assigned as +1) (*18*). To demonstrate a specific antisense effect, a random sequence, CAT CTA CGC TAC GTT TCT (PS-FANA), and a homopolymeric thymidine (18-mer) with 10 2′-deoxy-dT flanked by four araF-T, i.e., araF-(TTTT)-d(TTTTTTTTTT)-araF(TTTT), were also synthesized.

Measurement of CD Spectra and Melting Temperatures of Antisense/RNA Hybrids. UV thermal denaturation data

Table 1: Biophysical and Biological Properties of Phosphorothioate Antisense Oligonucleotides[a]

ID no.	oligomer sequence	DNA gap size	T_m (°C)[b]	k_{rel}[c]	EC_{50}[d] (nM)
	PS-DNA				
1	ATATCCTTGTCGTATCCC	0	62	1.00	150
	PS-FANA/Deoxy Chimeras				
2	ATATCCTTGTCGTATCCC	0	72	0.20	>500
3	ATATCCTTGTCGTATCCC	1	70	0.36	150
4	ATATCCTTGTCGTATCCC	4	69	0.32	10
5	ATATCCTTGTCGTATCCC	6	67	0.91	5
6	ATATCCTTGTCGTATCCC	8	64	1.75	5
7	ATATCCTTGTCGTATCCC	10	64	1.82	15
	2′-meRNA/Deoxy Chimeras				
8	AUAUCCUUGTCGUAUCCC	4	72	0.001	>500
9	AUAUCCTTGTCGUAUCCC	6	67	0. 23	>500
10	AUAUCCTTGTCGTAUCCC	8	68	0.87	25
11	AUAUCCTTGTCGTAUCCC	10	66	1.65	15

[a] The AON sequence is complementary to a coding region (+1056 to +1073) of luciferase mRNA. 2′-Deoxyribonucleotide residues are underlined. [b] T_m, melting temperature of the AON/RNA duplex. [c] Relative rate of *E. coli* RNase H mediated degradation of an 18 nt target RNA when duplexed to the AON (relative to rate observed for PS-DNA/RNA hybrid duplex). Data given are average values obtained from three independent experiments. Standard deviations were ≤5%. [d] Concentration of AON required to provide 50% inhibition of intracellular luciferase expression. Data given are average values obtained from two independent experiments.

were obtained on a Varian Cary 1 UV−vis spectrophotometer equipped with a Peltier temperature controller. Molar extinction coefficients for FANA oligomers were calculated using the nearest-neighbor approximation, and were assumed to be the same as those of DNA strands (*15*). Oligomers were mixed in equimolar ratios in 140 mM K^+, 1 mM Mg^{2+}, and 5 mM Na_2HPO_4 buffer, pH 7.2. The total duplex concentration was ca. 5 μM. Samples were heated to 80−90 °C for 15 min, then cooled slowly to room temperature, and stored at 4 °C overnight before measurements. Absorbance values were recorded after equilibration as the temperature was increased by 0.5 °C increments at 1 min intervals. T_m values were calculated using the baseline method and generally have an uncertainty of ±0.5 °C.

CD spectra were collected at 5 °C on a Jasco J-710 spectropolarimeter at a rate of 100 nm/min using fused quartz cells. Measurements were carried out in 140 mM K^+, 1 mM Mg^{2+}, and 5 mM Na_2HPO_4 buffer, pH 7.2, at a duplex concentration of 5 μM.

Purification of E. coli RNase H1. *E. coli* BL21 (DE3) pLys cells transformed with plasmid pET-21c/*rnhA*, which contains the RNase H gene (*rnhA*) of *E. coli*, were induced to overproduce RNase H with 1 mM isopropyl-β-thiogalactopyranoside (IPTG). The plasmid was a gift from Dr. J. Gaspar (University of Waterloo). Cell pellets were suspended in 50 mM Tris, pH 7.9, 0.2 M KCl, 5 mM $MgCl_2$, 0.1 mM EDTA, 1 mM 2-mercaptoethanol, and lysed by addition of Nonidet P40 (NP-40), a nonionic surfactant. The RNase H in the soluble fraction was purified as described previously (*19*).

In Vitro RNase H1 Assays. To prepare substrates for RNase H assays, the antisense oligonucleotide (10 pmol) and a 5′-^{32}P-labeled complementary RNA target (5 pmol) were mixed in a buffer (50 μL final) containing 60 mM Tris·HCl (pH 7.8), 60 mM KCl, 2.5 mM $MgCl_2$, 2 mM dithiothreitol, and 2 units of RNA guard RNase inhibitor (Amersham Pharmacia Biotech, Piscataway, NJ), then heated at 90 °C for 2 min and slowly cooled to room temperature to allow duplex formation. The substrate solutions were further incubated for at least 1 h at 37 °C prior to initiation of the assay by the addition of 0.1 nM purified *E. coli* RNase H1. Aliquots were removed at various times and quenched by the addition of an equal volume of denaturing loading buffer (98% deionized formamide, 10 mM EDTA, 1 mg/mL bromophenol blue, and 1 mg/mL xylene cyanol). Reaction products were denatured by heating at 100 °C for 5 min, followed by electrophoretic resolution on 16% polyacrylamide sequencing gels containing 7 M urea and visualization by autoradiography. Product formation was quantified by densitometry.

Effect of Antisense Oligonucleotides on Cellular Gene Expression. The HeLa X1/5 cell line (European Collection of Cell Cultures, Salisbury, U.K.) is stably transfected with the luciferase gene and expresses a functional luciferase enzyme (*20*, *21*). Cells were cultured in Dulbecco's modified Eagle's medium (DMEM) supplemented with 10% fetal bovine serum (FBS). Cells were seeded either in 96-well plates [at (1.5−2) × 10^4 cells/well] or in 6-well plates (at 5 × 10^5 cells/well). Antisense experiments were carried out 24 h after seeding, by which time cells were 80% confluent. Oligonucleotides were delivered to the cells using cytofectin GSV GS3815 (Glen Research, Sterling, VA) (*21*, *22*) according to the manufacturer's protocol. Briefly, oligonucleotides and cytofectin GSV were diluted with DMEM without serum to a 10× final concentration and 25 μg/mL, respectively. Equal volumes of oligonucleotide and cytofectin solutions were mixed in polystyrene plastic tubes and incubated for 15 min at room temperature, followed by the addition of 5 volumes of DMEM containing 10% FBS. The cell culture medium was replaced with the oligonucleotide/cytofectin mixture, and cells were incubated for 24 h before analysis. Cell viability was assessed following exposure to antisense oligonucleotides using a colorimetric XTT formazan dye assay.

Assay for Luciferase Activity. Luciferase activity assays were performed using the luciferase assay system (Promega, Madison, WI) according to the manufacturer's protocol. Briefly, following exposure to antisense molecules, cells were washed with phosphate-buffered saline and lysed, and aliquots were mixed with luciferin substrate solution. The resulting luminescence was immediately measured using a SPECTRAmax GEMINI XS microplate spectrofluorometer (Molecular Devices, Sunnyvale, CA) set at luminescence reading mode.

Determination of Luciferase Protein Expression. Aliquots of X1/5 cell lysates were centrifuged, and the protein content of individual samples was measured using Bio-Rad protein assay reagents (Bio-Rad, Hercules, CA). Equivalent amounts of total cell protein (10 μg) were resolved by SDS−PAGE, and then transferred to nitrocellulose. Luciferase protein levels were determined by immunoblot analysis using a goat anti-luciferase antibody (Chemicon International, Inc., Temecula, CA) and horseradish peroxidase-conjugated rabbit anti-goat IgG (Chemicon International, Inc.). Immunoblots were visualized using the Renaissance Western blot Chemiluminescence Reagent Kit (NEN Life Sciences, Boston, MA) according to the manufacturers' instructions.

Determination of Luciferase mRNA Expression. Total RNA from X1/5 cells was isolated, and luciferase mRNA levels were determined by Northern blot analysis according to standard methods (*23*). Briefly, equivalent amounts of total RNA (20 μg) were size-fractionated on 1% agarose gels containing 2.2 M formaldehyde, and then transferred to nitrocellulose membranes. Luciferase mRNA was probed with ^{32}P-internally-labeled DNA generated using an oligo-labeling kit (Amersham Pharmacia Biotech, Piscataway, NJ) and plasmid pGEM-Luc (Promega, Madison, WI) which contains full-length firefly luciferase cDNA. Radioactive signals were detected by autoradiography and quantified by densitometry. As an internal control for RNA loading, the membranes were stripped with boiling 1% SDS and then rehybridized with a probe for glyceraldehyde-3-phosphate dehydrogenase (GAPDH).

RESULTS

To evaluate the ability of 2′-deoxy-2′-fluoroarabinonucleic acids (FANA) to inhibit gene expression in cells, we synthesized phosphorothioate oligomers comprised solely of 2′-deoxy-2′-fluoroarabinonucleotides (PS-FANA) as well as chimeras containing both 2′-deoxy-2′-fluoroarabinonucleotides and 2′-deoxyribonucleotides, i.e., PS-[FANA-DNA-FANA] (Table 1). All oligomers were tested for hybridization affinity (T_m measurements), ability to direct target RNA cleavage by bacterial RNase H, and antisense activity in cultured human X1/5 cells.

Stability and Helical Conformation of AON/RNA Chimeric Duplexes. Table 1 summarizes the melting temperatures (T_m values), determined by ultraviolet (UV) spectroscopy, of hybrids of AONs bound to RNA using near-physiological buffer conditions. While T_m analysis of AON/RNA duplexes is not a measure of AON hybridization and dissociation rates at physiological conditions, it does provide useful information about the impact that 2′-*O*-methylribo and 2′-fluoroarabino substitutions have on duplex formation. The data show that the 18 bp PS-FANA/RNA hybrid (72 °C) is more stable than the corresponding PS-DNA/RNA hybrid (62 °C) (ΔT_m/bp = ca. +0.5 °C). This is consistent with the finding that phosphodiester (PO)-linked FANA/RNA hybrids are more stable than PO-DNA/RNA hybrids (ΔT_m/bp = ca. +1 °C) (*15*). With PS-FANA strands containing DNA gaps, hybrids show a thermal stability that is intermediate between that of PS-DNA/RNA and PS-FANA/RNA hybrids. The observed increase in melting temperature for a given oligonucleotide chimera correlated directly with the 2′-*O*-methylribose or 2′-fluoroarabinose content. This is exemplified by the data for the listed duplexes (Table 1). As 2′-*O*-methylribose or 2′-fluoroarabinose modifications were replaced with 2′-deoxynucleosides, T_m values were reduced by approximately 0.5−1.0 °C/deoxy substitution. These observations are in agreement with previous reports showing that 2′-meRNA and FANA oligomers bind RNA with higher affinity than uniform oligodeoxynucleotides (DNA) (*8*, *15*). Of note, the melting temperatures of the hybrids containing 2′-fluoroarabinose modifications are the same, or only slightly lower, than those of hybrids containing 2′-*O*-methylribose.

CD spectral analysis was used to establish whether the incorporation of 2′-fluoroarabinose and 2′-*O*-methylribose sugars within DNA has a fundamental influence on the conformation of the duplex structure. Therefore, a comparison was made between the CD spectra of chimeric hybrids containing 2′-fluoroarabinose and the analogous hybrids having 2′-*O*-methylriboses (Figure 2A). An intense positive CD band around 260 nm, a band of low intensity at 225 nm, and a strong negative band around 210 nm characterize the CD spectra of AON/RNA hybrids containing the 2′-fluoroarabino modifications. The positive band at 260 nm shifts slightly to longer wavelength with decreasing DNA gap size (Figure 2A). The overall spectral features very closely resemble those of A-form pure RNA/RNA duplexes. Since the CD spectra are all very similar, we conclude that all complexes have the same (A-like) geometry irrespective of the DNA gap size. This observation is consistent with the notion that 2′-fluoroarabinonucleotides are structurally and conformationally similar to the native 2′-deoxyribonucleotide units (*17*, *24*) and so would not expect to perturb the overall macromolecular architecture to any appreciable degreee. Indeed, recent NMR structure analysis carried out on FANA/RNA and DNA/RNA hybrids revealed a strong resemblance in terms of both the helical geometry (minor groove width) and the sugar puckers (*17*). In contrast, the CD spectra of the AON/RNA hybrids formed by 2′-*O*-methyl chimeric compounds are less alike (e.g., note amplitude changes at 264 nm), indicating that their respective structures are more dependent on the length of the DNA core (e.g., 4 deoxy versus 10 deoxy core size; Figure 2B). This is expected given that 2′-deoxyribonucleotides are characterized by C2′/O4′-*endo* sugars while 2′-*O*-methylribonucleotides are characterized by a C3′-*endo* antipodal preference. In summary, the CD studies indicate that the conformation of chimeric AON/RNA hybrids is relatively unaffected when 2′-fluoroarabinucleotides are substituted for DNA residues; however, 2′-meRNA to DNA substitutions significantly perturb the conformation of the helical structure.

RNase H Activity of 2′-Fluoroarabino/Deoxy Gap Oligonucleotides. Studies using backbone-modified chimeric oligonucleotides suggest that there is a correlation between antisense activity and the efficacy with which AONs elicit RNase H activity (*9*, *25*, *26*). We recently showed that RNase H can cleave an oligo-RNA strand in a hybrid that is hybridized to a complementary (PO)-FANA strand (*14*). To determine if PS-FANA and chimeric oligomers also support an RNase H-dependent mechanism of inhibition, these compounds were tested for their ability to activate *E. coli* RNase H1 in vitro (Figure 3). The data show that *all* compounds were capable of directing RNase H cleavage of target RNA at low enzyme concentration (Table 1 and Figure 3A). We also found that uniform PS-FANA is able to elicit RNase H activity, although the overall efficiency of RNA cleavage observed is significantly reduced (5-fold) relative to PS-DNA (Table 1). RNase H cleavage efficiency improved as deoxyribonucleotide residues were introduced in the center of the sequence; in fact, 2′-fluoroarabino chimeras containing 8 and 10 deoxy residues were more efficient at directing RNase H cleavage relative to PS-DNA (full deoxy). The locations of cleavage sites were very similar in all duplexes, but differences in cleavage preferences were noted (Figure 3B).

The effects of 2′-*O*-methyl modifications on the rate of RNase H cleavage were also determined by gel analysis

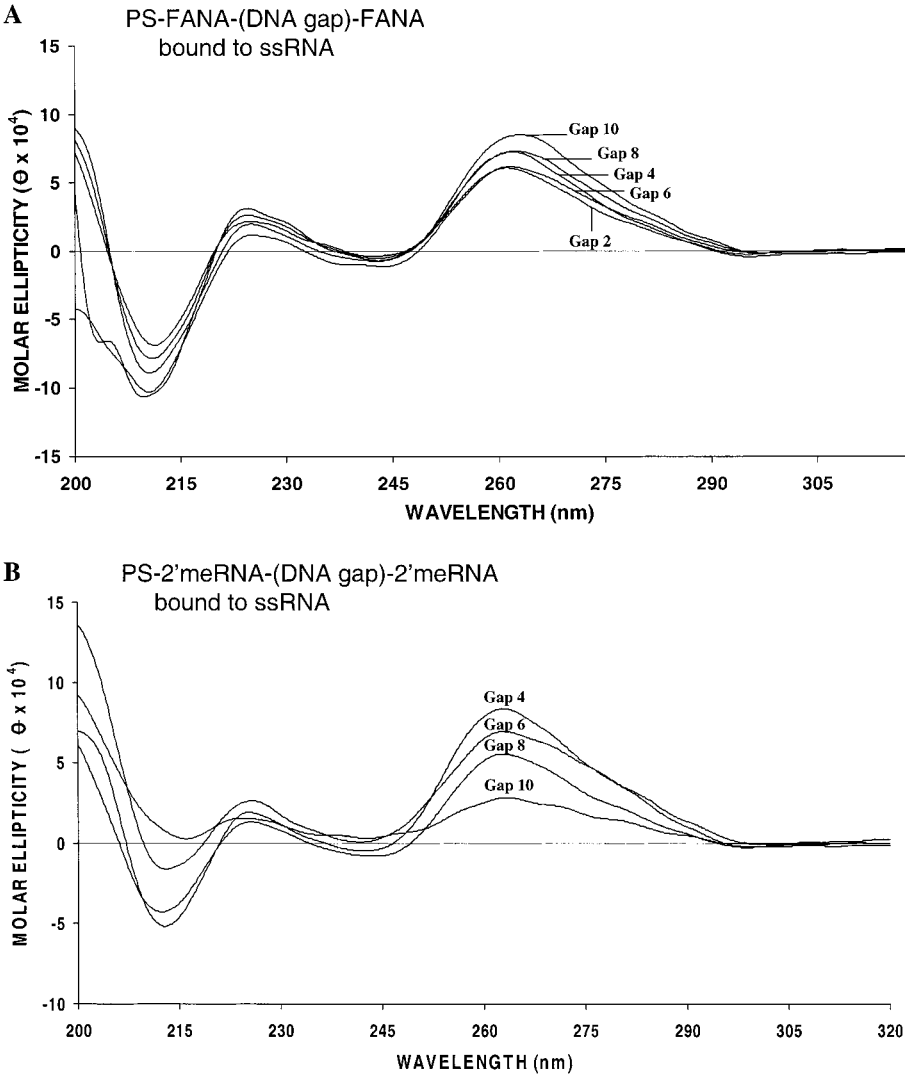

FIGURE 2: (A) CD spectra of hybrids in 140 mM K^+, 1 mM Mg^{2+}, and 5 mM Na_2HPO_4 buffer (pH 7.2). The total duplex concentration was ca. 5 μM. (A) RNA hybridized to PS-[FANA-DNA-FANA] chimeras having different gap size (sequences **3**−**7**, Table 1). (B) RNA hybridized to PS-[2′meRNA-DNA-2′meRNA] chimeras having different gap size (sequences **8**−**11**, Table 1).

(Table 1). Only the 2′meRNA/deoxy chimeras with relatively long DNA gaps (10 and 8 nucleotides) were able to elicit RNase H activity efficiently. As expected, RNA cleavage occurs primarily at sites complementary to the DNA gap (Figure 3B). In contrast, with the PS-[FANA-DNA-FANA]/RNA hybrids, cleavage also occurs at RNA regions hybridized to the PS-FANA segment (Figure 3B). Decreasing the DNA gap core of the 2′meRNA/deoxy chimeras to 6 and 4 nucleotides resulted in 5-fold and 30-fold decreases, respectively, in RNase H cleavage efficiency. Indeed, virtually no cleavage was observed with the 2′meRNA/deoxy chimera containing a DNA core of 4 deoxy residues. These results are in agreement with those reported by Inoue et al. (*8*) and confirm that *E. coli* RNase H1 has a minimum recognition requirement of 4 deoxy residues in a chimeric 2′meRNA/deoxy oligonucleotide. It is also worth noting that while PS-FANA (full arabino)/RNA hybrids are substrates of RNase H, hybrids of RNA and complementary 2′meRNA (full ribo) are not (*8*).

Antisense Activities of PS-[FANA-DNA-FANA] Chimeras. Next we determined the antisense potency and specificity of 2′-fluoroarabino deoxy gap oligomers in cell cultures. Specifically, we used a previously described HeLa X1/5 cell line, which stably expresses luciferase, to assess the ability of the FANA-base compounds to regulate the intracellular levels of the luciferase mRNA target (*18*). The corresponding PS-DNA (full deoxy) and 2′meRNA/deoxy chimeras were also synthesized for comparison. Oligonucleotides were delivered to the cells using the cationic lipid Cytofectin GSV GS3815 (*21*, *22*).

Dose−response curves for the various oligonucleotides and control sequences are shown in Figure 4A,B (EC_{50} values are tabulated in Table 1). The range of the doses was from 1 to 250 nM of antisense and control AONs. Treatment of cells with PS-DNA resulted in reduction of luciferase activity in a concentration-dependent manner with an EC_{50} of ca. 150 nM (Table 1). Significant decreases in intracellular luciferase activity were observed in cells treated with the 2′-fluoroarabino/deoxy chimeras. The data show that they are 15−30-fold more potent than the corresponding antisense PS-DNA. In some cases, nearly complete inhibition of luciferase enzyme activity (> 80%) was demonstrated at AON concentrations of 30 nM (Figure 4A). The EC_{50} of the most active 2′-fluoroarabiono/deoxy chimeras (6 and 8 deoxy gap) is 5 nM. Both PS-[$araFT_4$-dT_{10}-$araFT_4$] and "PS-FANA random" (a compound of the same base composition

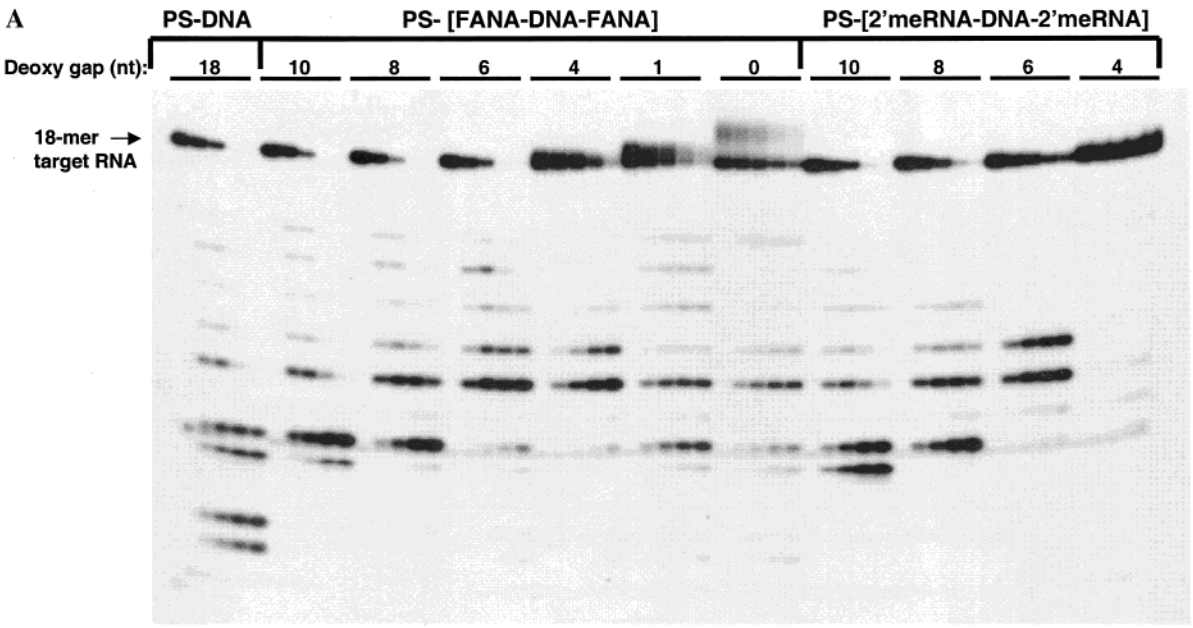

B *No gap*

```
        3'- U A U A G G A A C A G C A U A G G G -5'
S-DNA         *  *  *  *  ^    ^  ^  ^  ^
S-FANA        *  *  *  *  ^    ^  *  *  *
```

10 nt DNA gap

```
        3'- U A U A G G A A C A G C A U A G G G -5'
F             *  *  *  *  ^    ^  ^  *  *
M                *  *  *  ^    ^  ^
```

8 nt DNA gap

```
        3'- U A U A G G A A C A G C A U A G G G -5'
F             *  *  *  *  ^  *  ^  *  *  *
M                *  *  ^  *  ^  *
```

6 nt DNA gap

```
        3'- U A U A G G A A C A G C A U A G G G -5'
F             *  *  *  ^  ^  *  *  *  *  *
M                      ^  ^  *  *
```

4 nt DNA gap

```
        3'- U A U A G G A A C A G C A U A G G G -5'
F             *  *  *  ^  ^  *  *  *  *  *
M                         *  *  *
```

1 nt DNA gap

```
        3'- U A U A G G A A C A G C A U A G G G -5'
F             *  *  *  *  ^  *  ^  *  *  *
```

FIGURE 3: RNase H mediated cleavage of RNA duplexed with various antisense oligonucleotides. (A) Electrophoretic analysis of ^{32}P-labeled RNA digestion products. Timed aliquots were taken at 0, 5, 10, 20, and 30 min from each set of incubation as described under Materials and Methods. (B) Diagram of RNase H cleavage pattern. The sequences shown are those of the RNA target. The letters F and M represent PS-[FANA-DNA-FANA] and PS-[2′meRNA-DNA-2′meRNA] chimeras, respectively. RNA residues hybridized to the DNA gap residues are underlined. (∧) Major cut; (*) minor cut.

as **2**, but of random sequence; see Table 1) were virtually inactive, suggesting that the reduction of luciferase enzyme activities was predominantly due to an antisense effect (Figure 4B).

A dramatic decrease in antisense activity was observed for the uniform PS-FANA oligomer; in this case, the EC_{50} was >500 nM, an activity that was not distinguishable from those of the PS-DNA or "PS-FANA random" sequences. Remarkably, incorporation of only two (noncontiguous) dG residues within PS-FANA (sequence **3**, Table 1) leads to a significant increase in the potency of the AON (Table 1).

The relationship between antisense potency and intracellular levels of luciferase protein and mRNA is shown in Figure 4C,D. As can be seen, the potency of the 2′-fluoroarabino/deoxy chimera (10 deoxy gap) is superior to that of PS-DNA (full deoxy), and the luciferase activity correlates closely with mRNA and protein levels. The levels of a housekeeping mRNA GAPDH remained constant upon AON treatment, and the AONs tested did not affect X1/5 cell viability (>95%) up to a concentration of 500 nM. The two smaller RNA fragments (1.6 and 1.1 kb) migrating faster on the gels are consistent with an antisense-directed RNase

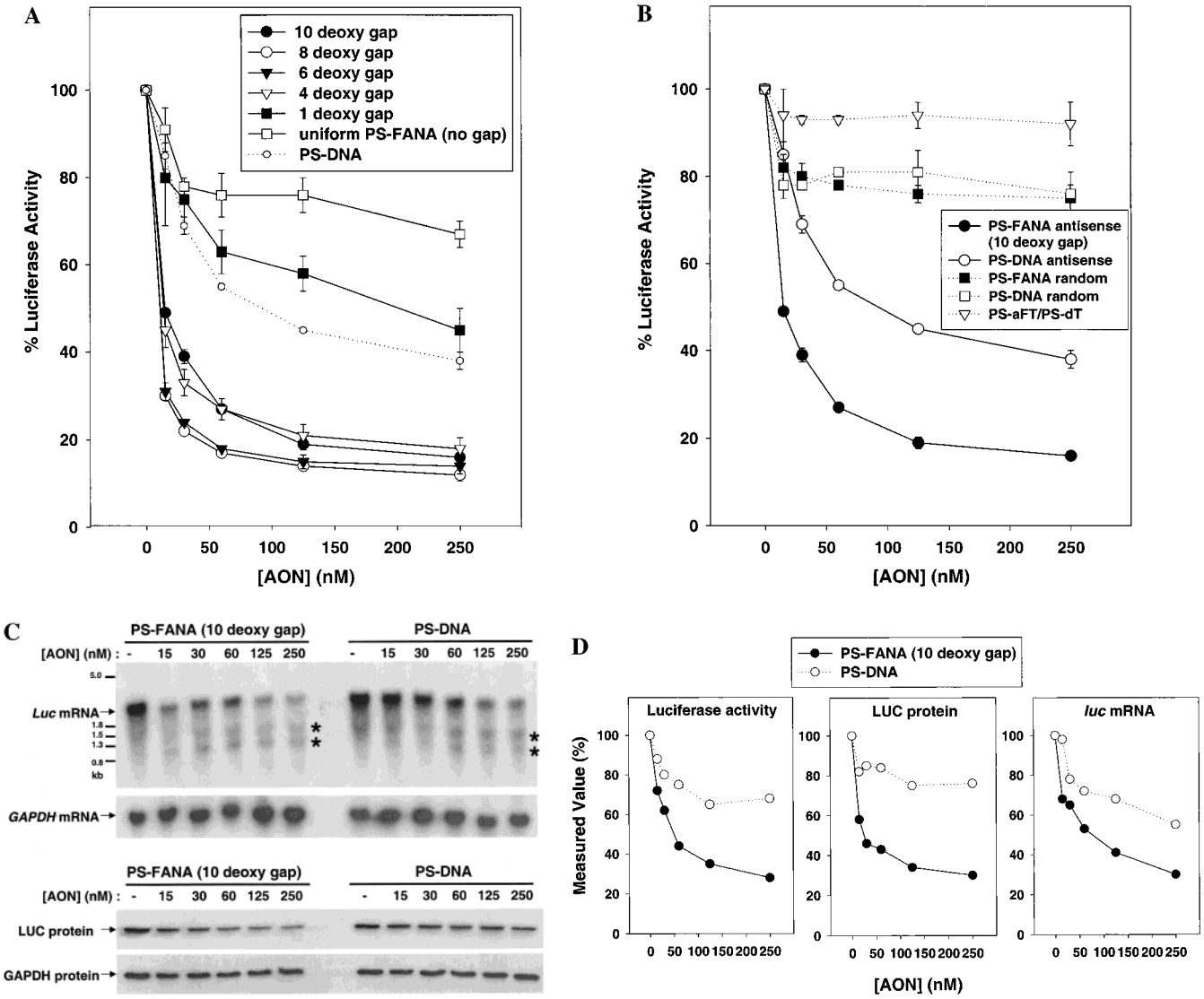

FIGURE 4: Sequence-specific antisense inhibition of chimeric oligonucleotides. X1/5 cells were transfected with 0−250 nM of the indicated antisense or random oligonucleotides complexed with cytofectin as described under Materials and Methods, and the luciferase expression was measured after 24 h. (A) Dose−response relationships of the effects of PS-[FANA-DNA-FANA] chimeras of various DNA gap composition on luciferase activities. (B) Comparison of effects of antisense and random sequences. The base sequence of the "random" oligomer is given under Materials and Methods. "PS-aFT/PS-dT" denotes the oligomer: araF-TTTT-(dTTTTTTTTTT)-araF-TTTT. (C) Comparison of the effects of PS-[FANA-DNA-FANA] (10 deoxy gap) and PS-DNA on levels of luciferase mRNA (Northern blot), protein (immunoblot), and luciferase activities measured simultaneously in a single experiment. The symbols "*" indicate the position of the expected RNA fragments resulting from AON-specific binding and RNase H mediated cleavage of luciferase mRNA. The levels of housekeeping GAPDH are shown for assessment of loading and specificity of inhibition by AONs. (D) Plot of quantitative data from (C).

H mediated cleavage of the recombinant 2.7 kb luciferase mRNA (Figure 4C).

Antisense Activities of PS-[FANA-DNA-FANA] versus PS-[2′meRNA-DNA-2′meRNA]. The experiments described above allow for a direct comparison of antisense activities of PS-[FANA-DNA-FANA] versus PS-[2′meRNA-DNA-2′meRNA] oligonucleotides. Direct comparison of dose−response curves for chimeric compounds with the same DNA gap size showed that the antisense potencies of the 2′-fluoroarabino/deoxy chimeras were in general significantly better than the corresponding 2′-meRNA/deoxy chimeras (Figure 5A,B and Table 1). Chimeric 2′meRNA oligonucleotides containing relatively long deoxy gaps, like their 2′-fluoroarabino/deoxy counterparts, displayed better inhibitory activities than that of PS-DNA (full deoxy) oligonucleotide (Figure 5A,B and Table 1). The most active PS-[2′meRNA-DNA-2′meRNA] compounds were the 10 and 8 deoxy chimeras. The 2′meRNA chimeras with the 6 and 4 deoxy gap displayed much weaker activity than the corresponding 2′-fluoroarabino compounds (Figure 5A, Table 1). As a whole, the most potent AONs tested were the PS-[FANA-DNA-FANA] chimeras containing 6 and 8 deoxynucleotides (EC_{50} = 5 nM). Figure 5C shows the effects of various AONs on the levels of luciferase mRNA and protein. A direct correlation between reduced levels of luciferase mRNA (and protein) and enzyme activity was observed for both series of compounds.

DISCUSSION

Recent advances such as (i) the development of efficient methods for the solid-phase synthesis of oligonucleotides (*27*−*29*), (ii) the use of mixed-backbone oligonucleotides that induce RNase H activity (*8*−*13*), and (iii) the develop-

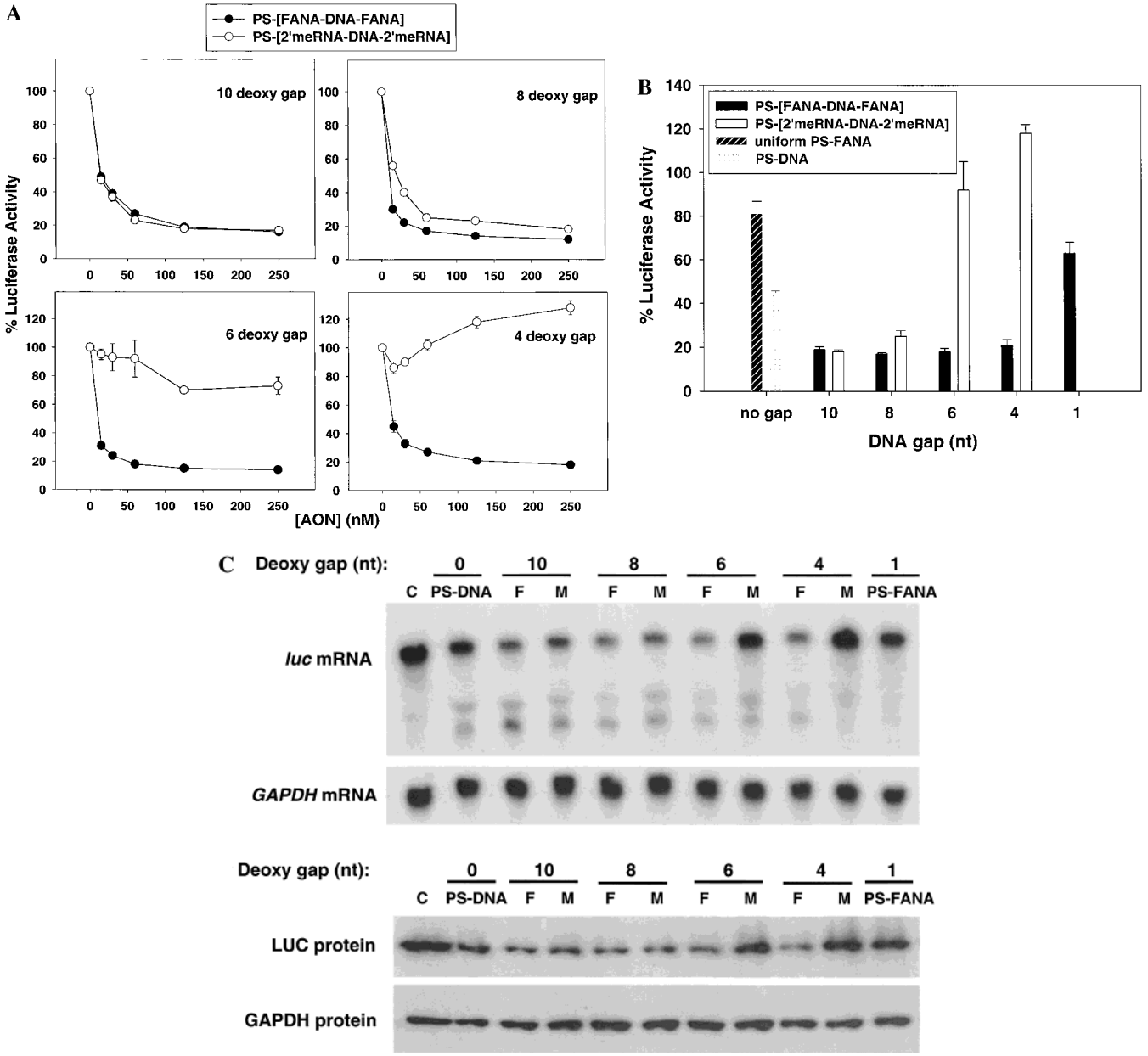

FIGURE 5: Comparative antisense effects of PS-[FANA-DNA-FANA] versus PS-[2′meRNA-DNA-2′meRNA] chimeras. (A) Dose−response inhibition of luciferase in HeLa X1/5 cells using PS-[FANA-DNA-FANA] (sequences **3**−**7**, Table 1) and PS-[2′meRNA-DNA-2′meRNA] chimeras (sequences **8**−**11**, Table 1). A range of concentrations (1−250 nM) was delivered to the HeLa cells using cytofectin. Extracts were prepared 24 h later and assayed for luciferase activity. (B) Bar diagram depicting luciferase activity measured at 250 nM [AON]. The *y*-axis gives luciferase activity expressed as percent relative to luciferase activity in the absence of AON (control). (C) The effects of AON chimeras (250 nM) on mRNA and protein levels. Lanes C, control experiment with no AON added; lanes F, PS-[FANA-DNA-FANA] chimera; lanes M, PS-[2′meRNA-DNA-2′meRNA] chimera.

ment of cationic lipids to efficiently deliver AONs to cells (*21*, *22*) have overcome many of the barriers limiting the use of AONs in biological systems. Indeed, several clinical trials using mixed-backbone AONs have been initiated for several human diseases including cancer, viral infections, and inflammatory afflictions. One remaining challenge, however, is the need to develop AONs that combine specificity and high mRNA affinity, while retaining the ability to activate RNase H. The latter requirement is particularly important since RNase H potentiates the biological activity of AONs, by degrading the mRNA portion of the AON/mRNA duplex, and releasing ('recycling') the AON (*5*, *11*).

We have previously described the synthesis and preliminary characterization of 2′-deoxy-2′-fluoroarabinonucleic acid (FANA) (*14*, *15*). These compounds represent the first example of a 2′-modified AON that induces RNase H activity while exhibiting high binding affinity for target RNA. FANA and its phosphorothioate derivative (PS-FANA) provide respectively +1.2 and +0.5 °C increase in binding affinity per modification compared to PS-DNA (e.g., see Table 1). While FANA has a weaker RNA affinity compared to its epimeric 2′F-RNA (*30*) and other 2′-modified RNAs (*6*), only FANA elicits RNase H activity when bound to the target RNA. Thus, although 2′-substituted RNA analogues have certain desirable properties, the fact that they do not elicit RNase H activity limits their usefulness as antisense agents. This disadvantage may be overcome by creating chimeric oligonucleotides composed of mixed 2′-*O*-substituted RNA

and a DNA 'gap' positioned in the middle of the sequence. These studies have shown that the minimum DNA gap size required to direct efficient RNase H cleavage of a target RNA is four to five residues (*8*, *9*), although more are required to confer significant biological activity in vitro and in vivo (*9*). In fact, most of the mixed-backbone oligonucleotides in clinical trials possess DNA gaps having a minimum of eight residues.

In an effort to assess the antisense properties of FANA oligonucleotides, we synthesized a series of FANA compounds containing phosphorothioate (PS) internucleotide linkages. Our reasoning for incorporating PS linkages in the backbone was 2-fold. First, PS linkages would confer better nuclease resistance and cellular uptake to the AON, and, second, they would allow direct comparison between FANA and the most widely used antisense compounds, i.e., chimeric PS-[2′meRNA-DNA-2′meRNA]. Thus, we prepared a series of octadecanucleotides, namely, PS-FANA, PS-DNA, and chimeric PS-[FANA-DNA-FANA] strands. The length of the DNA segment of the chimeras varied from 1 to 10 nucleotides, with the FANA segment length adjusted accordingly to keep the overall length of the chimeric compound fixed (18 nt). For comparison, we also evaluated the antisense properties of the corresponding chimeric PS-[2′meRNA-DNA-2′meRNA] strands.

As expected, the 2′meRNA and 2′F-arabino modifications were found to increase duplex stability, with the 2′-substituent content correlating directly with target affinity (Table 1). It is important to note that the binding affinity of a given PS-[2′meRNA-DNA-2′meRNA] chimera is very similar to the corresponding PS-[FANA-DNA-FANA] chimera. T_m values of hybrids formed by the 2′-fluoroarabino compounds were only 2−3 °C lower than those formed by the corresponding 2′-*O*-methylribose compounds. Thus, any observed differences in biological activity would likely not be due to differences in the binding affinity of these oligonucleotides.

Our results showed that the uniformly modified PS-FANA oligonucleotide was somewhat less efficient in directing RNase H cleavage of target RNA compared to the corresponding PS-DNA compound, and showed only weak antisense inhibition of cellular target expression (i.e., luciferase mRNA translation). However, the mixed-backbone PS-[FANA-DNA-FANA] oligonucleotides were found to possess potent antisense activity, inhibiting specific cellular gene expression with EC_{50} values of less than 5 nM. This inhibition was a true antisense effect, as indicated by the dose-dependent decrease in both target protein and target mRNA, and the appearance of mRNA fragments consistent with RNase H mediated cleavage of the mRNA target.

A significant finding of this study is that while the antisense potency of the 2′-*O*-methyl/deoxy compounds was dramatically attenuated with decreasing DNA core size, that of the 2′-fluoroarabino/deoxy compounds was essentially unaffected (Figure 5A−C). In fact, the 2′-fluoroarabino/deoxy chimera with two (noncontiguous) dG residues retained significant antisense activity (Figure 5A,B). These findings correlated exactly with the ability of the various chimeric antisense oligonucleotides to elicit RNase H degradation of the target RNA, strongly suggesting that RNase H degradation of target RNA, and not binding affinity, is the most important determinant for potent antisense activity. As predicted, the cleavage induced by PS-[2′meRNA-DNA-2′meRNA] chimeras was restricted to the RNA portion bound to the DNA gap (Figure 3). In contrast, distribution of initial cleavage sites induced by PS-FANA and the PS-[FANA-DNA-FANA] chimeras occurred through the entire RNA chain. While subtle differences in cleavage patterns were observed for the different FANA chimeras, it appeared that the duplexes were cleaved similarly.

Differences in nuclease stability and/or cellular uptake may also explain the observed differences in antisense activities of the 2′-*O*-methyl/deoxy versus FANA/deoxy chimeras containing small gaps. Although we have not compared the nuclease stability of both types of chimeras, we note that PS-FANA and PS-DNA have comparable stability in human serum (stable for at least 24 h with negligible amount of $n-1$ product in both cases). In addition, we have found that while the antisense activity of PS-DNA declined after 24 h with gradual recovery of luciferase expression, that of PS-FANA/deoxy and PS-2′-meRNA/deoxy chimeras (8 deoxy gap) presisted up to 60 h with much slower rebound of luciferase activity (C.-N. Lok, M. J. Damha, and M. A. Parniak, unpublished results). These experiments suggest that both type of chimeras are very stable in the cell culture media.

The recently solved NMR structure of a FANA/RNA hybrid (*17*) along with the CD studies described in the present report provide an explanation for several of the observations made in this study. The NMR study showed that FANA/RNA hybrids adopt a structure that resembles that of native DNA/RNA hybrids (*17*). In addition to their "hybrid" (H)-like conformation, there are other important structural features that are conserved in both hybrids. The sugars of the RNA strand have a normal C3′-*endo* (north) conformation, whereas the FANA (and DNA) sugars adopt a unique O4′-*endo* (east) conformation (*17*, *24*). Notably, the minor groove width is slightly narrower in both DNA/RNA and FANA/RNA hybrid duplexes (9 Å) than in pure RNA/RNA species (11 Å). A minor groove width that is intermediate between those of pure A- and B-form duplexes is believed to be an important factor in the mechanism that allows RNase H to discriminate between DNA/RNA and RNA/RNA duplexes (*31*). The striking similarities between FANA/RNA and the native DNA/RNA substrate explain why FANA/RNA duplexes invoke RNase H activity. It is not surprising, therefore, that PS-FANA (fully substituted) and chimeras containing both 2′-fluoroarabino (FANA) and deoxynucleotide (DNA) residues behave as 'DNA mimics' and invoke cleavage of the RNA through most of the ribonucleotide sequence (Figure 3). CD measurements indeed showed that the "hybrid" (H) conformation of the AON/RNA duplexes is relatively unaffected when 2′-fluoroarabinocleotides are substituted for DNA residues (Figure 2A). On the other hand, 2′-modified *ribo*nucleotides (e.g., 2′F, 2′OMe, 2′MOE RNA) with the opposite stereochemistry at C2′ show a strong preference for a C3′-*endo* (north) conformation (*32* and cited literature). Preorganization of the AON into a pure C3′-*endo* (north) conformation produces a pure A-form AON/RNA duplex that is not cleaved by RNase H. Therefore, use of combinations of north (ribo) and east/south (DNA) residues in the same strand would be disruptive because they are expected to introduce A/H junctions along the AON/RNA duplex (Figure 6). This is consistent with

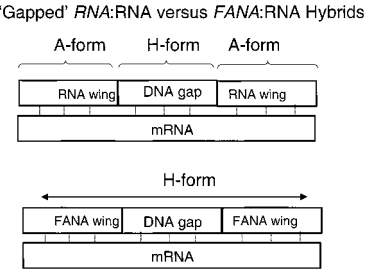

FIGURE 6: Schematic representation chimeric hybrid duplexes. Hybrids of RNA and 2′meRNA/deoxy chimeras are comprised of "A-H-A" conformational domains, whereas those between RNA and 2′-fluoroarabino/deoxy chimeras belong to the "H" conformational family.

the CD data shown in Figure 2B, which provide evidence that DNA to 2′-meRNA substitutions significantly perturb the conformation of the hybrid structure. In such "A-H-A" hybrid constructs, the "A" segment (2′meRNA) serves solely as a target-binding domain to ensure effective hybridization, whereas the "H" core (DNA) serves as an RNase H activation domain that confines the cleavage to a limited site on the target RNA.

While DNA/RNA and FANA/RNA hybrids have many conformational features in common, there are some differences when examined in sufficient detail. Combined analyses of NOE and *J*-coupling data have indicated that the 2′-fluoroarabino sugars are conformationally 'rigid' and adopt almost exclusively the O4′-*endo* pucker (*17*, *24*). This contrasts strongly with the 'dynamic' sugar conformation previously observed in the DNA strands of DNA/RNA hybrid duplexes, where a mixture of conformers likely coexist (O4′, C2′, and C3′-*endo*) (*17*, *33*, and cited literature). The energy barrier for interconversion between FANA sugar conformers is higher due to the large gauche effect from the strongly electronegative 2′-fluorine atom and the furanose ring oxygen (O4′). According to this analysis, and those reported by Marquez and co-workers, the increased stability of FANA/RNA hybrids relative to DNA/RNA hybrids could originate from the conformational preorganization of the sugar moieties and the ordering of water molecules around the fluorine atoms (*17*, *34*). The greater conformational freedom ('flexibility') of 2-deoxyribose relative to 2-fluoroarabinose sugars may account, at least in part, for the faster rate of cleavage generally observed for DNA/RNA hybrids relative to PS-FANA/RNA (Table 1) and PO-FANA/RNA hybrid duplexes [e.g., when the base sequence of the AON is ATATCCTTGTCGTATCCC, the PO-DNA/RNA duplex is cleaved by *E. coli* RNase H twice as fast relative to the corresponding PO-FANA/RNA duplex; C.-N. Lok, E. Viazovkina, C. J. Wilds, K.-L. Min, M. A. Parniak, and M. J. Damha, unpublished results]. Although we have no formal proof of this hypothesis, we note that the rate of RNase H cleavage nearly doubles upon incorporation of two (noncontiguous) dG residues in the center of the chimera (Table 1). This finding may provide new insights into the design of future AON analogues.

The two major criteria considered to be important for antisense activity are the strength of binding of the AON to the target RNA (T_m) and the ability of the AON/RNA duplex to be recognized and cleaved by RNase H (*5*, *8*, *9*). The T_m values for the PS-[FANA-DNA-FANA] chimeras were similar to or slightly lower than those for the corresponding PS-[2′meRNA-DNA-2′meRNA] chimeric antisense, for each of the DNA core gap sizes tested (Table 1). The dramatic differences in antisense activity of the PS-[FANA-DNA-FANA] compared to the corresponding PS-[2′meRNA-DNA-2′meRNA] chimeras, when the DNA gap size was 6 residues or less, provide strong evidence that the inhibitory activity of AON results primarily from the RNase H mediated cleavage of the mRNA target when hybridized to the AON. Thus, it appears that the ability of an antisense oligonucleotide to elicit RNase H degradation of the complementary target mRNA is likely to be the single most important determinant for the inhibitory potency of antisense oligonucleotides.

ACKNOWLEDGMENT

We thank Ms. Maria Mangos for her assistance in the preparation of the manuscript.

REFERENCES

1. Crooke, S. T. (2000) *Methods Enzymol. 313*, 3−45.
2. Agrawal, S., and Kandimalla, E. R. (2000) *Mol. Med. Today 6*, 72−81.
3. Stein, C. A. (1999) *Nat. Biotechnol. 17*, 209.
4. Zamecnik, P. C., and Stephenson, M. L. (1978) *Proc. Natl. Acad. Sci. U.S.A. 75*, 280−284.
5. Walder, R. Y., and Walder, J. A. (1988) *Proc. Natl. Acad. Sci. U.S.A. 85*, 5011−5015.
6. Manoharan, M. (1999) *Biochim. Biophys. Acta 1489*, 117−130.
7. Kawasaki, A. M., Casper, M. D., Freier, S. M., Lesnik, E. A., Zounes, M. C., Cummins, L. L., Gonzalez, C., and Cook, P. D. (1993) *J. Med. Chem. 36*, 831−841.
8. Inoue, H., Hayase, Y., Iwai, S., and Ohtsuka, E. (1987) *FEBS Lett. 215*, 327−330.
9. Monia, B. P., Lesnik, E. A., Gonzalez, C., Lima, W. F., McGee, D., Guinosso, C. J., Kawasaki, A. M., Cook, P. D., and Freier, S. M. (1993) *J. Biol. Chem. 268*, 14514−14522.
10. Crooke, S. T., Lemonidis, K. M., Neilson, L., Griffey, R., Lesnik, E. A., and Monia, B. P. (1995) *Biochem. J. 312 (Pt. 2)*, 599−608.
11. Lima, W. F., and Crooke, S. T. (1997) *Biochemistry 36*, 390−398.
12. Zhou, W., and Agrawal, S. (1998) *Bioorg. Med. Chem. Lett. 8*, 3269−3274.
13. McKay, R. A., Cummins, L. L., Graham, M. J., Lesnik, E. A., Owens, S. R., Winniman, M., and Dean, N. M. (1996) *Nucleic Acids Res. 24*, 411−417.
14. Damha, M. J., Wilds, C. J., Noronha, A., Bruckner, I., Borkow, G., and Parniak, M. A. (1998) *J. Am. Chem. Soc. 120*, 12976−12977.
15. Wilds, C. J., and Damha, M. J. (2000) *Nucleic Acids Res. 28*, 3625−3635.
16. Noronha, A. M., Wilds, C. J., Lok, C. N., Viazovkina, K., Arion, D., Parniak, M. A., and Damha, M. J. (2000) *Biochemistry 39*, 7050−7062.
17. Trempe, J.-F., Wilds, C. J., Denisov, A., Pon, R. T., Damha, M. J., and Gehring, K. (2001) *J. Am. Chem. Soc. 123*, 4896−4903.
18. de Wet, J. R., Wood, K. V., DeLuca, M., Helinski, D. R., and Subramani, S. (1987) *Mol. Cell. Biol. 7*, 725−737.
19. Yang, W., Hendrickson, W. A., Kalman, E. T., and Crouch, R. J. (1990) *J. Biol. Chem. 265*, 13553−13559
20. Gossen, M., and Bujard, H. (1992) *Proc. Natl. Acad. Sci. U.S.A. 89*, 5547−5551.
21. Flanagan, W. M., Kothavale, A., and Wagner, R. W. (1996) *Nucleic Acids Res. 24*, 2936−2941.
22. Lewis, J. G., Lin, K. Y., Kothavale, A., Flanagan, W. M., Matteucci, M. D., DePrince, R. B., Mook, R. A., Jr., Hendren, R. W., and Wagner, R. W. (1996) *Proc. Natl. Acad. Sci. U.S.A. 93*, 3176−3181.

23. Ausbel, F. M., Brent, R., Kingston, R. E., Moore, D. D., Smith, J. A., Seidman, J. G., and Struhl, K. (1995) *Current Protocols in Molecular Biology*, John Wiley and Sons, New York.
24. Berger, I., Tereshko, V., Ikeda, H., Marquez, V. E., and Egli, M. (1998) *Nucleic Acids Res. 26*, 2473−2480.
25. Flanagan, W. M., Wolf, J. J., Olson, P., Grant, D., Lin, K. Y., Wagner, R. W., and Matteucci, M. D. (1999) *Proc. Natl. Acad. Sci. U.S.A. 96*, 3513−3518.
26. Gutierrez, A. J., Matteucci, M. D., Grant, D., Matsumura, S., Wagner, R. W., and Froehler, B. C. (1997) *Biochemistry 36*, 743−748.
27. Letsinger, R. L., and Lunsford, W. B. (1976) *J. Am. Chem. Soc. 98*, 3655−3661.
28. Beaucage, S. L., and Caruthers, M. H. (1981) *Tetrahedron Lett. 22*, 1859−1862.
29. Ogilvie, K. K., Usman, N., Nicoghosian, J., and Cedergren, R. J. (1988) *Proc. Natl. Acad. Sci. U.S.A. 85*, 5764−5768.
30. Wilds, C. J. (2000) Ph.D. Thesis, McGill University.
31. Federoff, O., Salazar, M., and Reid, B. R. (1993) *J. Mol. Biol. 233*, 509−523.
32. Teplova, M., Minasov, G., Tereshko, V., Inamati, G. B., Cook, P. D., Manoharan, M., and Egli, M. (1999) *Nat. Struct. Biol. 6*, 535−539.
33. Cheatham, T. E., III, and Kollman, P. A. (1997) *J. Am. Chem. Soc. 119*, 4805−4825.
34. Ikeda, H., Fernandez, R., Wilk, A., Barchi, J. J., Jr., and Marquez, V. E. (1998) *Nucleic Acids Res. 26*, 2237−2244.

BI0115075